The Astrophysical Journal, 816:100 (6pp), 2016 January 10 doi:10.3847/0004-637X/816/2/100

REVEALING W51C AS A COSMIC RAY SOURCE USING *FERMI*-LAT DATA

T. Jogler[1,2] and S. Funk[1,2]
[1] W. W. Hansen Experimental Physics Laboratory, Kavli Institute for Particle Astrophysics and Cosmology, Department of Physics and SLAC National Accelerator Laboratory, Stanford University, Stanford, CA 94305, USA; jogler@slac.stanford.edu
[2] Erlangen Centre for Astroparticle Physics, D-91058 Erlangen, Germany
Received 2015 November 17; accepted 2015 November 27; published 2016 January 14

ABSTRACT

Supernova remnants (SNRs) are commonly believed to be the primary sources of Galactic cosmic rays. Despite intensive study of the non-thermal emission of many SNRs the identification of the accelerated particle type relies heavily on assumptions of ambient-medium parameters that are only loosely constrained. Compelling evidence of hadronic acceleration can be provided by detecting a strong roll-off in the secondary γ-ray spectrum below the π^0 production threshold energy of about 135 MeV, the so called "pion bump." Here we use five years of *Fermi*-Large Area Telescope data to study the spectrum above 60 MeV of the middle-aged SNR W51C. A clear break in the power-law γ-ray spectrum at $E_{\rm break} = 290 \pm 20$ MeV is detected with 9σ significance and we show that this break is most likely associated with the energy production threshold of π^0mesons. A high-energy break in the γ-ray spectrum at about 2.7 GeV is found with 7.5σ significance. The spectral index at energies beyond this second break is $\Gamma_2 = 2.52^{+0.06}_{-0.07}$ and closely matches the spectral index derived by the MAGIC Collaboration above 75 GeV. Therefore our analysis provides strong evidence to explain the γ-ray spectrum of W51C by a single particle population of protons with a momentum spectrum best described by a broken power law with break momentum $p_{\rm break} \sim 80$ GeV/c. W51C is the third middle-aged SNR that displays compelling evidence for cosmic-ray acceleration and thus strengthens the case of SNRs as the main source of Galactic cosmic rays.

Key words: astroparticle physics – gamma-rays: general – ISM: supernova remnants

1. INTRODUCTION

Supernova remnants (SNRs) are widely believed to be the sources of Galactic cosmic rays ($E < 10^{15}$ eV). Verification of this hypothesis is possible by studying the γ-ray emission from SNRs. Accelerated cosmic rays interact with surrounding matter and produce π^0mesons that subsequently decay into γ-rays, leading to a characteristic break in the γ-ray spectrum at about $E \sim 200$–300 MeV due to the finite rest mass of the π^0. Competing leptonic γ-ray production mechanisms such as bremsstrahlung and inverse Compton (IC) emission require strong fine tuning to produce a similar feature.[3] The pion bump is thus an unmistakable feature of the hadronic origin of γ-ray emission that is observable by the *Fermi*-Large Area Telescope (LAT). This feature was recently found in the two brightest SNRs detected by *Fermi*-LAT, IC 443 and W44, as reported in Ackermann et al. (2013). The third brightest SNR detected by *Fermi*-LAT, W51C, is another prime candidate to search for the pion-decay signature in the γ-ray emission because it is interacting with a molecular cloud (MC) that poses an excellent target for cosmic-ray interactions and subsequent π^0 decay.

W51C is an SNR identified by its radio shell and assumed to be 30 kyr old and at a distance of 5.5 kpc (Sato et al. 2010). The SNR belongs to the larger W51 complex composed of one of the largest star-forming regions in our Galaxy and divided into two parts denoted W51A and W51B. The SNR is located toward the south-eastern end of W51B and evidence for interaction between the SNR shell and the MC W51B is provided by the discovery of two OH (1720 MHz) masers by Green et al. (1997). Further evidence is provided by high-velocity atomic gas that shows velocity shifts between 20 and 120 km s^{-1} with respect to the ambient medium (Koo & Moon 1997). The OH masers and the high-velocity clouds are commonly interpreted as the result of shock waves penetrating into MCs. More recent measurements by Ceccarelli et al. (2011) find an overabundance of overionized gas in certain W51B locations close to W51C that they interpret as the result of ionization through by-products of freshly accelerated cosmic rays interacting with nucleons. All these measurements outline a compelling scenario in which the SNR shell of W51C is interacting with the MC W51B.

X-ray imaging of the region revealed a hard source denoted CXO J192318.5+140305, which was identified as a possible pulsar wind nebula (PWN) related to the SNR (Koo et al. 2002, 2005). Such a PWN could also power relativistic particle acceleration resulting in γ-ray emission.

W51C was detected in 11 months of data by the *Fermi*-LAT and showed spatially extended γ-ray emission at $E > 2$ GeV. The γ-ray spectrum showed curvature that required a break at a few GeV, and subsequent modeling by a hadronic spectrum required a broken power law for the proton spectrum with a break momentum of 10–15 GeV/c (Abdo et al. 2009). At very high energies ($E > 100$ GeV, VHE) an energy-dependent morphology was revealed by the MAGIC Collaboration (Aleksić et al. 2012). No hint of spectral variation could be identified and the emission is attributed to the SNR W51C due to its morphology and multi-wavelength modeling of the spectral energy distribution (SED). The authors mention that a contribution of up to 20% of the W51C flux could come from the PWN candidate CXO J192318.5+140305. A final determination of the parent particle population that creates the γ-rays was not possible, though multi-wavelength interpretation of the SED of W51C favors a hadronic origin of the γ-ray emission.

[3] The break required in the right position of the lepton energy spectrum and the extremely hard spectral index, inexplicable by conventional diffuse shock acceleration, render leptonic-model explanations unlikely.

Here we analyze five years of *Fermi*-LAT data and search for features that can identify the parent particle type in the most detailed γ-ray spectrum of W51C derived to date.

2. OBSERVATIONS AND DATA ANALYSIS

The LAT, the primary instrument of the *Fermi Gamma-ray Space Telescope* mission, is a pair-conversion telescope sensitive to γ-rays in an energy range from 20 MeV to $E > 300$ GeV. The reader is referred to Atwood et al. (2009) for a more detailed description and to Ackermann et al. (2012) for the on-orbit performance. We analyzed public *Fermi*-LAT data between MJD 54682.7 and MJD 56516.5 corresponding to about five years of Pass 7 Reprocessed data. The data are analyzed using the `Fermi ScienceTools` version v9r32p04.[4] We select events with high probability of being γ-rays by choosing the SOURCE event class. In order to evade γ-ray contamination generated by cosmic rays hitting the Earth's atmosphere, we remove time intervals when the field of view of the LAT came too close to the Earth's limb (zenith angle $< 100°$). We analyze data between 60 MeV and 300 GeV and use the P7REP_SOURCE_V15 instrument response functions (IRFs). To account for the interstellar γ-ray emission caused by cosmic rays interacting with gas or interstellar radiation in our Galaxy, the model gll_iem_v05_rev1.fit is used. This interstellar emission model (IEM) is our standard IEM provided by the *Fermi*-LAT Collaboration for point-source analysis. The isotropic γ-ray emission is accounted for by the model iso_source_v05.txt, which also includes any residual charged-particle background present in the *Fermi*-LAT data. We chose a $20° \times 20°$ region of interest (ROI) centered on W51C and performed a binned likelihood analysis with $0\overset{\circ}{.}1$ bins and 30 bins logarithmically spaced in energy.

We construct a test statistic (TS) following Mattox et al. (1996) to evaluate the improvement of the likelihood fit to the ROI when adding a new source. In the case of one additional source with one additional free parameter we can define $\mathrm{TS} = 2(L - L_0)$ and the significance as $\sigma = \sqrt{\mathrm{TS}}$ where L_0 and L are the log-likelihood values without the source and with it respectively.

In order to study the effect of nearby sources on the spectral fit of W51C we use `gtobssim`[3] to obtain Monte Carlo simulations of the W51C region. In our simulations we assume spectral values for all sources as given in the 3FGL catalog (Acero et al. 2015a). We vary all independent spectral parameters randomly by either $+2\sigma$ or -2σ of the associated error. The $\pm 2\sigma$ is chosen to provide an estimation in the case of a strong deviation of the real spectral value from that in the 3FGL catalog and at the same time to require running only a few simulations. We run ten variations of the simulation so that different combinations of sources have positive and negative fluctuations. Afterwards we analyze these ten Monte Carlo simulation samples with varying free parameters for the likelihood fit of the background sources. Finally, we compare the fit results of W51C with the simulated values for each analysis. We find that we have only to leave free parameters of the five sources marked with cyan crosses in Figure 1 in the likelihood fit to obtain within statistical uncertainties the simulated parameter values of W51C. For sources with

[4] Both the data and the associated software packages along with the templates used to model the interstellar and extragalactic emission are made publicly available by the *Fermi* Science Support Center at http://fermi.gsfc.nasa.gov/ssc/data/.

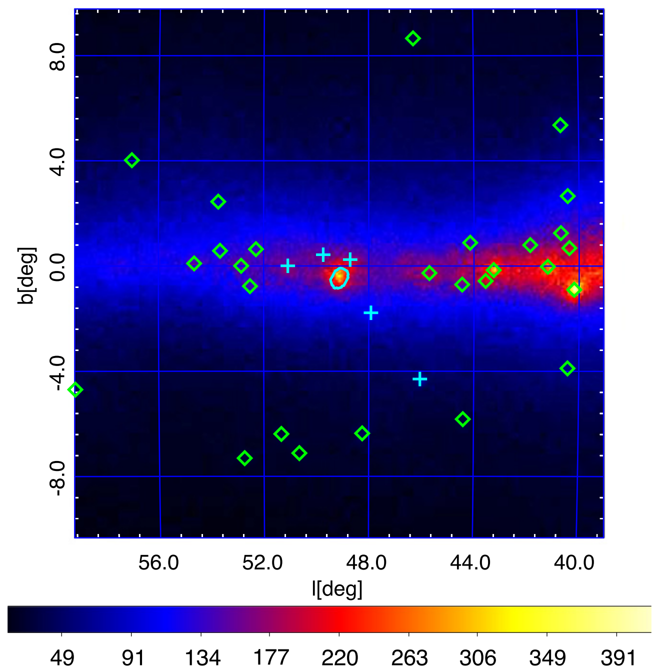

Figure 1. Map of photon counts above 60 MeV for the five years of *Fermi*-LAT data. Sources with spectral parameters left free in the likelihood fit are shown as cyan crosses and all other sources as green diamonds. The W51C template contour is the cyan ellipse in the center. W51C is the brightest source in the central part of the ROI.

TS < 50 in the 3FGL catalog we leave only the normalization free, and for more significant sources all other independent spectral parameters too. In addition to the sources in Figure 1 we also leave free the normalizations of the IEM and the isotropic emission template in our analysis.

To estimate the systematic uncertainties on flux and spectral properties of W51C caused by our limited knowledge of the IEM we compare the standard IEM results with the results obtained with eight alternative models generated with GALPROP (Vladimirov et al. 2011) and afterwards refined by fitting to the *Fermi*-LAT data. Each of these models consists of eight map cubes (i.e., three-dimensional models of gamma-ray intensity as a function of position and energy) inferring the interstellar γ-ray emission from gas by tracing it with H I and CO maps. The H I and CO maps are divided into the contributions from four galactocentric rings. In addition to these contributions there are map cubes added for large residual structures in the *Fermi*-LAT γ-ray sky, namely Loop I (Casandjian et al. 2009), the *Fermi* bubbles (Su et al. 2010; Ackermann et al. 2014), and an IC emission map. For a more detailed explanation of the alternative models see Acero et al. (2015b). Inside the W51C ROI only the H I rings 2–4, the CO rings 2–4, the IC map, and the Loop I template give any background contribution and all other components are removed from our fits. In addition to these components an IEM-specific isotropic component is added.

In our IEM systematic uncertainty study the normalizations of the individual components of each IEM are free in the likelihood fit. The alternative IEMs provide more freedom to the fit by leaving the components individually adjustable

[5] For further information see http://fermi.gsfc.nasa.gov/ssc/data/analysis/scitools/obssim_tutorial.html

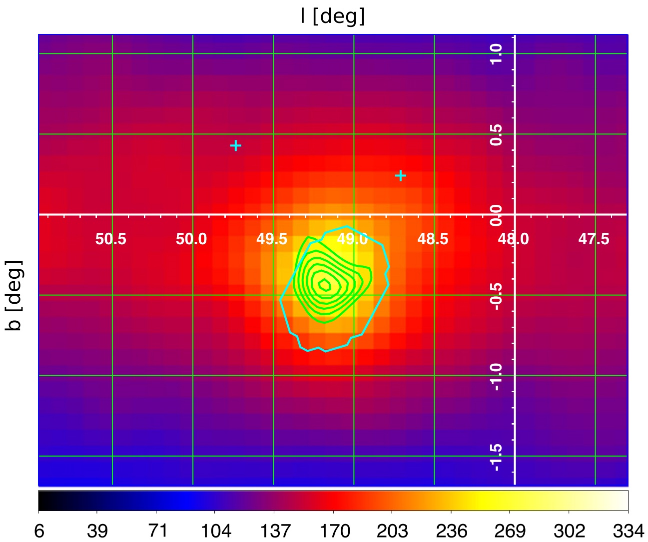

Figure 2. The *Fermi*-LAT map of photon counts of W51C above 60 MeV is shown as a color scale; overlaid are the *Fermi*-LAT W51C template in a cyan contour and the MAGIC W51C significance contours (Aleksić et al. 2012) above 150 GeV in green. Nearby *Fermi*-LAT sources from the 3FGL catalog are marked by crosses. The overlap of the two contours suggests that MAGIC and *Fermi*-LAT detect emission from the same region, while the broader PSF of *Fermi*-LAT at low energies makes more detailed comparisons impossible.

instead of only one global normalization, as in the case of the standard IEM .

3. THE W51C REGION AS SEEN BY *FERMI*-LAT

W51C was already reported to be an extended source for the *Fermi*-LAT in Abdo et al. (2009). We use the `pointlike` code (Kerr et al. 2011) to verify whether our data set, which is more than five times larger than that used in Abdo et al. (2009), would allow us to further constrain the morphology of W51C. Therefore we divide the γ-ray emission into energy bands from 60 MeV to 1 GeV, 1–5 GeV, and 5–300 GeV. The energy ranges are chosen to separate the individual spectral regimes present in the W51C γ-ray spectrum (see Section 4) and simultaneously include high photon statistics in each bin. No solid evidence for changing morphology between the tested energy bands is found. Slight differences in the position, geometry, and shape of the γ-ray excess that are seen between the individual energy bands have no impact on the obtained photon spectrum and thus are negligible for the spectral analysis of W51C. In our study W51C is modeled by a flat elliptical disk with five free parameters (R.A., decl., minor axis, major axis, rotation angle). In the best-position fit we use the best-fit spectral values obtained with the previously published template[6] and afterwards verify that leaving the spectral parameters free in the position fit does not alter the spatial shape or position. A fit using a two-dimensional Gaussian instead of the elliptical disk does not result in an improvement of the overall description of the region and has only insignificant effects on the W51C fit results. Our best-fit morphology for the overall energy range is in good agreement with the previously published template of W51C and we use this publicly available template for all our studies.

[6] Available from: http://fermi.gsfc.nasa.gov/ssc/data/analysis/LAT_essentials.html

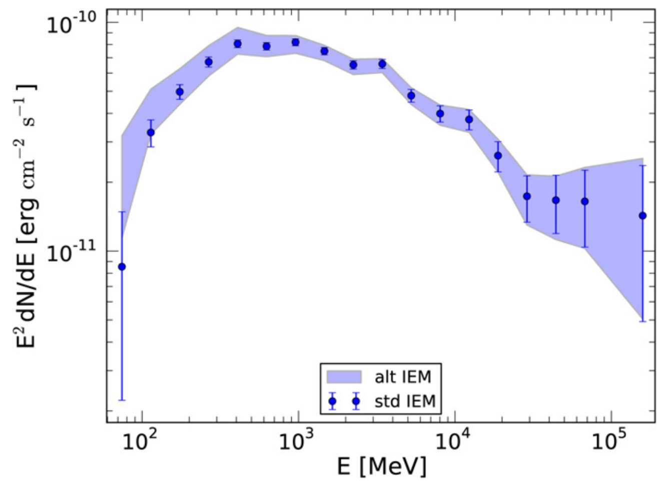

Figure 3. W51C SED as obtained from the *Fermi*-LAT data using the standard IEM (points). The envelope over all statistical error bars of the eight alternative IEM SEDs is shown by the blue band. A break in the SED around 300 MeV, as well as a second one at about 3 GeV, are clearly visible for all the IEMs used.

Comparing the morphology of W51C seen by the *Fermi*-LAT with that obtained by MAGIC shows a spatial coincidence as seen in Figure 2. The MAGIC contours are not an exact match to the *Fermi*-LAT template but they completely overlap. The difference between the two shapes might be explained by the lower angular resolution of the *Fermi*-LAT, making it impossible as shown in Lande et al. (2012) to distinguish between very similar source shapes. We conclude from these comparisons that the changes in energy-dependent morphology seen by MAGIC cannot be detected at $E < 75$ GeV by *Fermi*-LAT.

4. SEARCH FOR THE PION CUT-OFF IN W51C

We fit the W51C flux in 20 logarithmic energy bins independently between 60 MeV and 300 GeV. The resulting SED is shown in Figure 3 and a clear low-energy break around 300 MeV is visible. The SEDs obtained using the alternative IEMs differ by more than the statistical errors only at energies below a few GeV. All of them indicate a low-energy break at a very similar energy to the standard IEM. Above about 1 GeV there are only very small differences between the SEDs derived with the alternative IEMs and the standard one, as expected since the diffuse emission from cosmic-ray interactions decreases more rapidly than the source spectrum.

The significance of the break is obtained by fitting W51C using the likelihood approach between 60 MeV and 3 GeV once with a smoothly broken power law of the form $F(E) = N_0 (E/E_0)^{\Gamma_1} [1 + (E/E_{\rm break})^{(\Gamma_1 - \Gamma_2)/\alpha}]^{-\alpha}$, with $E_0 = 200$ MeV and $\alpha = 0.1$, and once with a power law of the form $F(E) = N_0 (E/E_0)^{-\Gamma}$. The improvement in likelihood when fitting a smoothly broken power law and assuming a nested model with two additional degrees of freedom yields a 9σ significance for a spectral break at $E_{\rm break} = 290 \pm 20$ MeV and change of spectral index from $\Gamma_1 = 0.70^{+0.23}_{-0.28}$ to $\Gamma_2 = 2.15 \pm 0.03$. To estimate the systematic uncertainty of the break energy due to our limited knowledge of the *Fermi*-LAT IRFs the bracketing IRFs method is used (Ackermann et al. 2012). Here the worst-case scenario, in which the IRFs change maximally at the break energy, is assumed to provide conservative systematic uncertainties. Additionally we apply the same method using the eight alternative IEMs and obtain very similar results for E_{break}. The alternative IEM fits allow us to estimate the systemaitc uncertainty of the break energy by calculating the variance with respect to the standard IEM (Acero et al. 2015b). Furthermore, the smoothly broken power law is favored above a power law in all alternative models and yields at least a significance of 8.7σ, rendering the break significant in all IEMs tested. The variation of the IEMs is currently our best method to estimate uncertainties associated with our limited knowledge of the IEM but cannot provide a complete coverage of all possible deviations. Taking into account the aforementioned uncertainties, we obtain a clear low-energy break in the W51C spectrum at $E_{\mathrm{break}} = 290 \pm 20(\mathrm{stat}) \pm 40(\mathrm{syst, IEM}) \pm 30(\mathrm{syst, IRF})$ MeV. In addition we also test for the effect of energy dispersion that results in general in an overprediction of the lowest flux point in the SED by about 30%. Similar to the study in Ackermann et al. (2013) we find that neglecting energy dispersion in our analysis leads to a lower significance of the detected low-energy break. The break in W51C shows very similar properties (E_{break}, Γ_1, Γ_2) to those of the SNRs W44 and IC 443 that were already identified convincingly as cosmic-ray accelerators (Ackermann et al. 2013).

Closer inspection of the W51C SED suggests that there is also a high-energy break in the spectrum. Indeed such a break is expected since the spectral index above the low-energy break, $\Gamma_2 = 2.15 \pm 0.03$, is not compatible with that obtained by the MAGIC Collaboration at energies beyond 75 GeV, $\Gamma = 2.58 \pm 0.07$ (Aleksić et al. 2012). Applying the same likelihood approach as for the low-energy break but using the energy range 400 MeV to 300 GeV to compare between smoothly broken power law and simple power law, we find a break at $E_{\mathrm{break,HE}} = 2.7^{+1.0}_{-0.8}(\mathrm{stat})$ GeV with 7.5 σ significance. Systematic uncertainties due to the IEM are unimportant at these energies and, given the large statistical uncertainty, all systematic errors are negligible in comparison. The power-law spectral index changes from $\Gamma_1 = 2.11^{+0.06}_{-0.05}$ in the low-energy regime to $\Gamma_2 = 2.52^{+0.06}_{-0.07}$ above the break. The high-energy spectral index is in excellent agreement with the spectral index reported by the MAGIC Collaboration at energies above 75 GeV, and thus the MAGIC spectrum can be well explained by the same particle population as the *Fermi* emission above $E_{\mathrm{break,HE}}$. In the next section the origin of the γ-ray emission is tested with hadronic and leptonic scenarios.

5. MODELING THE W51C SED

The obtained W51C SED is fitted by a proton-induced and alternatively by an electron-induced γ-ray spectrum. For the case of the electron-induced spectrum we consider IC- and bremsstrahlung-dominated γ-ray production. The γ-ray spectra for the leptonic cases are calculated according to the cross sections given in Blumenthal & Gould (1970) and Ellison et al. (1999) for electron–electron bremsstrahlung. The IC seed photons are provided by the cosmic microwave background (CMB), the emission of infrared light, mainly from dust, and starlight. Each of these seed photon fields is modeled by a blackbody spectrum with $kT_{\mathrm{CMB}} = 2.3 \times 10^{-4}$ eV, $u_{\mathrm{CMB}} = 0.26$ eV cm^{-3} for the CMB, $kT_{\mathrm{IR}} = 3 \times 10^{-3}$ eV, $u_{\mathrm{IR}} = 0.90$ eV cm^{-3} for infrared light, and $kT_{\mathrm{Star}} = 0.25$ eV, $u_{\mathrm{Star}} = 0.84$ eV cm^{-3} for starlight. The values are taken from Abdo et al. (2009). We also consider cooling effects due to synchrotron emission for electrons above 1 TeV, for which we assume a constant injection. Other cooling channels are unimportant for the assumed acceleration lifetime of the SNR (30 kyr) and are thus neglected. The proton–proton cross sections are taken from Kamae et al. (2006) and we multiply them by a factor of 1.85 to account for heavier element abundance as suggested by Mori et al. (2009). Secondary spectra from the decay of charged pions are computed as well but found to contribute insignificantly to the total γ-ray emission and hence are neglected.

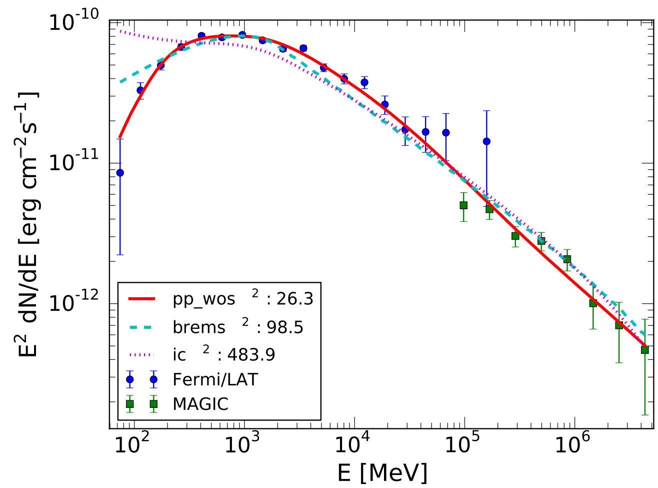

Figure 4. W51C SED as obtained from the *Fermi* data (blue points) and MAGIC data (green squares). The best-fit models for γ-ray emission induced by proton–proton interactions (solid red), bremsstrahlung (dashed cyan), and the IC effect (dotted magenta) are shown together with their χ^2 values. Only the proton–proton model describes the data reasonably.

For all tested processes the parent particle spectrum is modeled by a broken power law with an exponential cut-off in momentum space. A comparison with a simple power law with exponential cut-off yields much worse results for bremsstrahlung and IC processes and a slightly worse description in the case of the hadronic spectrum. We note that we use only statistical errors when fitting the SED.

The best-fit spectra are shown in Figure 4 and the only adequate description of the *Fermi*-LAT data is provided by the proton-induced emission spectrum. Including the MAGIC data in the fit yields again a valid description only with the proton spectrum with $(\chi^2/\mathrm{dof})_{\mathrm{pp}} = 26.3/22$, whereas the χ^2 values of the IC $(\chi^2/\mathrm{dof})_{\mathrm{IC}} = 484/23$ and bremsstrahlung spectra $(\chi^2/\mathrm{dof})_{\mathrm{Brems}} = 98.5/23$ indicate an insufficient description of the data. More complicated spectral shapes that allow for another low-energy break in the lepton spectrum might be able to explain the W51C spectrum as due to bremsstrahlung processes but again that would require strong fine tuning. Therefore we find the hadronic explanation of the γ-ray spectrum to be the most convincing model.

We also fitted the SEDs obtained using the alternative IEMs to assess the modeling dependence of the dominant systematic uncertainties with the aforementioned processes. The proton–proton mechanism is always significantly favored above the bremsstrahlung description.

The proton spectrum has a rather soft spectral index below the break of $\Gamma_1 = 2.48 \pm 0.02$ compared to the $\Gamma = 2.0$ or harder predicted by diffusive shock acceleration (DSA). However, we note that fixing the spectral index to $\Gamma = 2.0$ results in a worse but perhaps still acceptable value

$\chi^2/\mathrm{dof} = 47.8/23$. Also the two other SNRs, IC 443 and W44, that are identified as proton accelerators show rather soft spectral indices ($\Gamma = 2.36$) very similar to W51C.

We determine the break momentum to be $p_{\mathrm{break}} = 81.3^{+5.8}_{-5.4}$ GeV/c and the high-energy spectral index to be $\Gamma_2 = 2.73 \pm 0.03$. Our fit does not allow for a determination of the exponential cut-off; we find by profiling the cut-off momentum that any value between $p_{\mathrm{cut}} = 30$ TeV and $p_{\mathrm{cut}} = 300$ TeV yields $\Delta\chi^2 < 3.7$.

6. CONCLUSION

We establish a low-energy break at $E_{\mathrm{break}} = 290 \pm -20(\mathrm{stat}) \pm 40_{\mathrm{syst,IEM}} \pm 30_{\mathrm{syst,IRF}}$ MeV in the γ-ray spectrum of W51C. This break is associated with the energy threshold of π^0production and hence is strong evidence of the hadronic origin of the γ-ray emission. Furthermore, we establish a second break in the photon spectrum at $E_{\mathrm{break,HE}} = 2.7^{1.0}_{-0.8}(\mathrm{stat})$ GeV that smoothly connects the *Fermi*-LAT spectrum and the spectrum obtained by the MAGIC Collaboration above 75 GeV. The best description of the combined *Fermi*-LAT and MAGIC SED is given by a proton–proton-induced γ-ray spectrum with a broken-power-law spectrum in momentum space of the parent particles.

These results make W51C the third definitely identified SNR accelerating cosmic rays. As with the other two SNRs, IC 443 and W44, W51C is a middle-aged SNR that is not expected to contain the highest-energy cosmic rays it accelerated in its youth. All three of these objects require a broken power-law momentum spectrum of the protons. The break in the momentum spectrum is not connected to the π^0break in the γ-ray spectrum but is required to describe the high-energy part of W51C's γ-ray spectrum. The nature of the break in the parent particle population is unknown, but since there is no energy-dependent morphology found in the *Fermi*-LAT energy range[7] two independent proton particle populations seem unlikely to explain the break. According to models of cosmic-ray diffusion (Aharonian & Atoyan 1996; Gabici et al. 2009), the highest-energy cosmic rays start to escape from middle-aged SNRs, but this scenario results in an exponential cut-off in the parent particle spectrum and not a break. Such an exponential cut-off is not sufficient to model the W51C data or those of the other two SNRs. Another possible explanation for a break in the proton spectrum is a modification of the shock acceleration due to the interaction with the surrounding MC, maybe by neutral ion damping as suggested in Malkov et al. (2011) for the case of W44. Another possibility might be that emission is generated through reaccelerating existing cosmic rays in shocks in MCs triggered by SNR blast waves (Uchiyama et al. 2010). In this scenario a break could be observed as an overlay of different acceleration zones in the MC that have varying densities (Uchiyama et al. 2010). In the case of W51C there is evidence for interaction between the SNR shell and adjacent MCs from multi-wavelength data. Also in W44 there is evidence for interaction with surrounding MCs (Uchiyama et al. 2012). On the other hand IC 443 is most likely not directly interacting with an MC and there is some diffusion required before the cosmic rays can interact with the MCs in the vicinity of the SNR shock; hence models for escaping cosmic rays have been developed (Torres et al. 2010). The cause of the rather soft proton spectrum and the momentum break at a few to hundreds of GeV/c in these three SNRs cannot be conclusively explained at present. The differences in the environments of these three SNRs might explain the differences in the break momentum and the change in the spectral index, but our knowledge of the exact environmental parameters is limited. Interestingly, in all three cases an additional exponential cut-off in the γ-ray emission and in the parent particles is not detected. Therefore the highest-energy protons still accelerated by the SNR (or reaccelerated in the MCs) cannot be determined but must exceed about 30 TeV. Finding such high-energy protons in a relatively old SNR such as W51C is surprising, and future measurements with imaging Cherenkov telescopes, like the Cherenkov Telescope Array, will reveal the acceleration capabilities of W51C. Also more detailed morphology studies of W51C will help to provide further insight into what part of the MC–SNR interaction leads to modification of the cosmic-ray spectrum around the high-energy break and provide vital input to the development of theoretical models that will be able to explain the current data.

The *Fermi*-LAT Collaboration acknowledges generous ongoing support from a number of agencies and institutes that have supported both the development and the operation of the LAT as well as scientific data analysis. These include the National Aeronautics and Space Administration and the Department of Energy in the United States, the Commissariat à l'Energie Atomique and the Centre National de la Recherche Scientifique/Institut National de Physique Nucléaire et de Physique des Particules in France, the Agenzia Spaziale Italiana and the Istituto Nazionale di Fisica Nucleare in Italy, the Ministry of Education, Culture, Sports, Science and Technology (MEXT), High Energy Accelerator Research Organization (KEK), and Japan Aerospace Exploration Agency (JAXA) in Japan, and the K. A. Wallenberg Foundation, the Swedish Research Council, and the Swedish National Space Board in Sweden.

Additional support for science analysis during the operations phase is gratefully acknowledged from the Istituto Nazionale di Astrofisica in Italy and the Centre National d'Études Spatiales in France.

Facility: Fermi-(LAT).

REFERENCES

Abdo, A. A., Ackermann, M., Ajello, M., et al. 2009, ApJL, 706, L1
Acero, F., Ackermann, M., Ajello, M., et al. 2015a, ApJS, 218, 23
Acero, F., Ackermann, M., Ajello, M., et al. 2015b, ApJS, accepted
Ackermann, M., Ajello, M., Albert, A., et al. 2012, ApJS, 203, 4
Ackermann, M., Ajello, M., Allafort, A., et al. 2013, Sci, 339, 807
Ackermann, M., Albert, A., Atwood, W. B., et al. 2014, ApJ, 793, 64
Aharonian, F. A., & Atoyan, A. M. 1996, A&A, 309, 917
Aleksić, J., Alvarez, E. A., Antonelli, L. A., et al. 2012, A&A, 541, A13
Atwood, W. B., Abdo, A. A., Ackermann, M., et al. 2009, ApJ, 697, 1071
Baring, M. G., Ellison, D. C., Reynolds, S. P., Grenier, I. A., & Goret, P. 1999, ApJ, 513, 311
Blumenthal, G. R., & Gould, R. J. 1970, RvMP, 42, 237
Casandjian, J.-M., Grenier, I. & for the Fermi Large Area Telescope Collaboration 2009, arXiv:0912.3478
Ceccarelli, C., Hily-Blant, P., Montmerle, T., et al. 2011, ApJL, 740, L4
Gabici, S., Aharonian, F. A., & Casanova, S. 2009, MNRAS, 396, 1629
Green, A. J., Frail, D. A., Goss, W. M., & Otrupcek, R. 1997, AJ, 114, 2058
Kamae, T., Karlsson, N., Mizuno, T., Abe, T., & Koi, T. 2006, ApJ, 647, 692
Kerr, M. 2011, PhD Thesis, Univ. Washington

[7] There is strong evidence for an energy-dependent morphology in the MAGIC data but the break in the parent particle spectrum is already evident using only *Fermi*-LAT data.

Koo, B.-C., Lee, J.-J., & Seward, F. D. 2002, AJ, 123, 1629
Koo, B.-C., Lee, J.-J., Seward, F. D., & Moon, D.-S. 2005, ApJ, 633, 946
Koo, B.-C., & Moon, D.-S. 1997, ApJ, 475, 194
Lande, J., Ackermann, M., Allafort, A., et al. 2012, ApJ, 756, 5
Malkov, M. A., Diamond, P. H., & Sagdeev, R. Z. 2011, NatCo, 2, 194
Mattox, J. R., Bertsch, D. L., Chiang, J., et al. 1996, ApJ, 461, 396
Mori, M. 2009, APh, 31, 341
Sato, M., Reid, M. J., Brunthaler, A., & Menten, K. M. 2010, ApJ, 720, 1055
Su, M., Slatyer, T. R., & Finkbeiner, D. P. 2010, ApJ, 724, 1044
Torres, D. F., Marrero, A. Y. R., & de Cea Del Pozo, E. 2010, MNRAS, 408, 1257
Uchiyama, Y., Blandford, R. D., Funk, S., Tajima, H., & Tanaka, T. 2010, ApJL, 723, L122
Uchiyama, Y., Funk, S., Katagiri, H., et al. 2012, ApJL, 749, L35
Vladimirov, A. E., Digel, S. W., Jóhannesson, G., et al. 2011, CoPhC, 182, 1156